Peptides 87 (2017) 20–27

Contents lists available at ScienceDirect

Peptides

journal homepage: www.elsevier.com/locate/peptides

Region-specific bioconversion of dynorphin neuropeptide detected by *in situ* histochemistry and MALDI imaging mass spectrometry

Erik Bivehed[a], Robert Strömvall[a], Jonas Bergquist[b], Georgy Bakalkin[a], Malin Andersson[a,*]

[a] Department of Pharmaceutical Biosciences, Uppsala University, Uppsala 751 24, Sweden
[b] Department of Chemistry—BMC, Analytical Chemistry and SciLifeLab, Uppsala University, Uppsala 751 24, Sweden

ARTICLE INFO

Article history:
Received 28 February 2016
Received in revised form 6 October 2016
Accepted 9 November 2016
Available online 10 November 2016

Keywords:
Neuropeptide
Dynorphin
Bioconversion
Enzyme
Enzyme inhibitor
Histochemistry
MALDI imaging mass spectrometry
Mass spectrometry
Parkinson's disease
Neuropathic pain

ABSTRACT

Brain region-specific expression of proteolytic enzymes can control the biological activity of endogenous neuropeptides and has recently been targeted for the development of novel drugs, for neuropathic pain, cancer, and Parkinson's disease. Rapid and sensitive analytical methods to profile modulators of enzymatic activity are important for finding effective inhibitors with high therapeutic value.

Combination of *in situ* enzyme histochemistry with MALDI imaging mass spectrometry allowed developing a highly sensitive method for analysis of brain-area specific neuropeptide conversion of synthetic and endogenous neuropeptides, and for selection of peptidase inhibitors that differentially target conversion enzymes at specific anatomical sites. Conversion and degradation products of Dynorphin B as model neuropeptide and effects of peptidase inhibitors applied to native brain tissue sections were analyzed at different brain locations. Synthetic dynorphin B (2 pmol) was found to be converted to the N-terminal fragments on brain sections whereas fewer C-terminal fragments were detected. *N*-ethylmaleimide (NEM), a non-selective inhibitor of cysteine peptidases, almost completely blocked the conversion of dynorphin B to dynorphin B(1–6; Leu-Enk-Arg), (1–9), (2–13), and (7–13). Proteinase inhibitor cocktail, and also incubation with acetic acid displayed similar results.

Bioconversion of synthetic dynorphin B was region-specific producing dynorphin B(1–7) in the cortex and dynorphin B (2–13) in the striatum. Enzyme inhibitors showed region- and enzyme-specific inhibition of dynorphin bioconversion. Both phosphoramidon (inhibitor of the known dynorphin converting enzyme neprilysin) and opiorphin (inhibitor of neprilysin and aminopeptidase N) blocked cortical bioconversion to dynorphin B(1–7), wheras only opiorphin blocked striatal bioconversion to dynorphin B(2–13).

This method may impact the development of novel therapies with aim to strengthen the effects of endogenous neuropeptides under pathological conditions such as chronic pain. Combining histochemistry and MALDI imaging MS is a powerful and sensitive tool for the study of inhibition of enzyme activity directly in native tissue sections.

1. Introduction

It is often desirable to screen enzyme activity in complex sample matrices, such as tissues, as this can give biologically more relevant data than *in vitro* assays. Neuropeptides are often involved in several different processes engaging different brain regions (example opioid neuropeptides: reward, pain, movement control, *etc.*); thus agonist/antagonist have often displayed unwanted side-effects as other areas than intended are affected. For example, for opioid peptides the need to alleviate pain is also associated with a risk of developing drug dependence. Therefore, it is highly desirable to find region-specific targets whenever this is possible. In particular brain enzymes often display characteristic expression patterns confined to distinct areas, for example the mouse angiotensin-converting enzyme is strongly localized to the striatum, globus pallidus, and substantia nigra of the basal ganglia [1]. The lateral striatum has been shown to express high levels of prodynorphin mRNA

Abbreviations: IMS, imaging mass spectrometry; DA, dopamine; PD, Parkinson's disease; LID, L-DOPA-induced dyskinesia; NEM, *N*-Ethylmaleimide; DynB, dynorphin B.

* Corresponding author at: Uppsala University, Department of Pharmaceutical Biosciences, Box 591, SE-751 24 Uppsala, Sweden.
E-mail address: Malin.Andersson@farmbio.uu.se (M. Andersson).

http://dx.doi.org/10.1016/j.peptides.2016.11.006

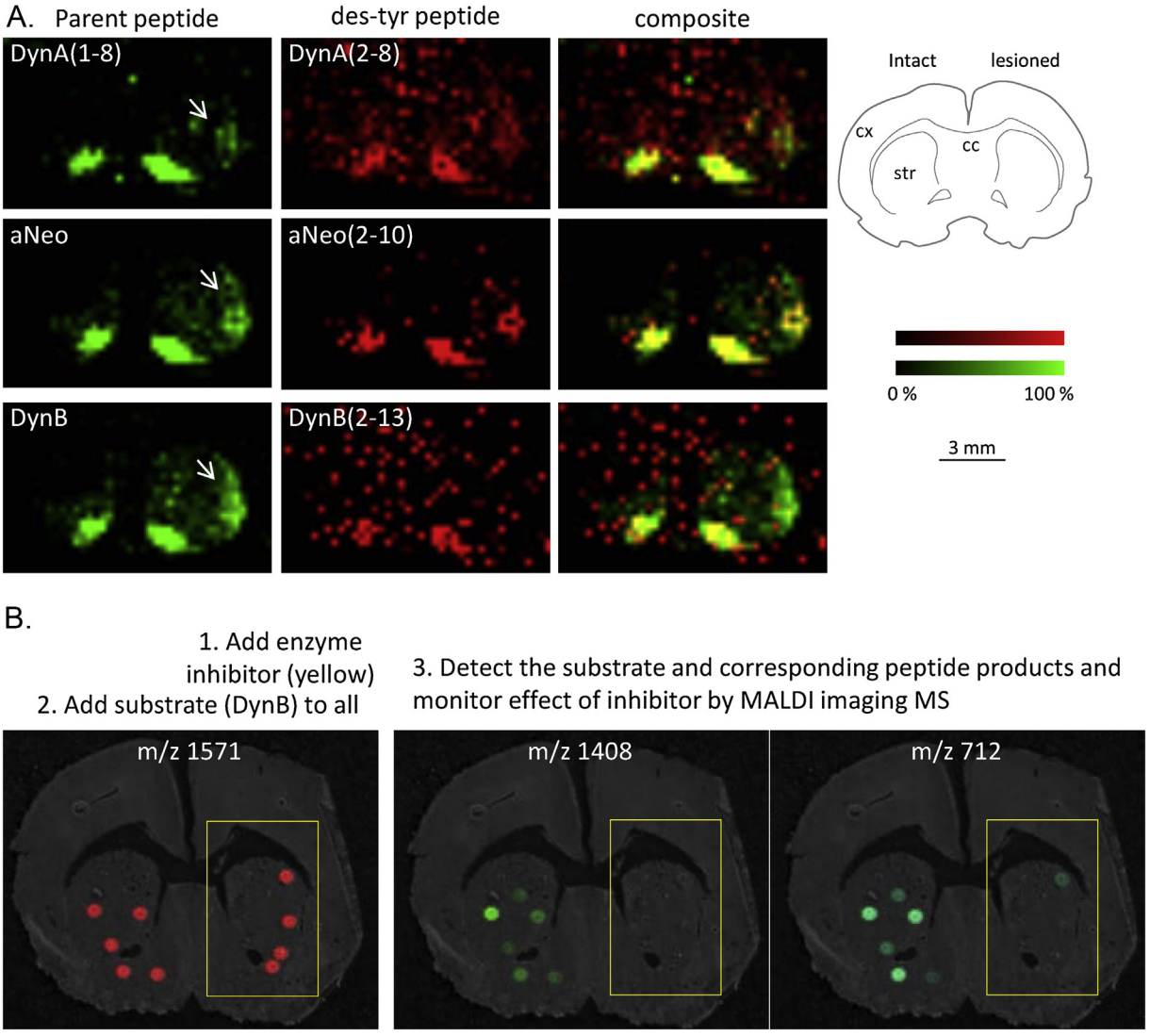

Fig. 1. Localized bioconversion in disease model and experimental set-up. (A) MALDI imaging MS of endogenous dynorphins in experimental Parkinson's disease (PD). The rat model of PD use a unilateral injection of 6-hydroxydopamine to produce a dopamine denervated striatum (to the right side in images), whereas the contralateral striatum is left intact. After L-DOPA-treatment some subjects develop abnormal involuntary movements that are similar to dyskinesia in PD patients. The severity of dyskinesia is positively correlates to the levels of dynorphin neuropeptides, predominantly dynorphin B (DynB), alpha-neoendorphin (aNeo), and aNeo(2–8)(arrows). The des-tyrosinated dynorphins were only up-regulated in the striatum, but not in other areas such as the substantia nigra (not shown) [4,5]. Modified from Hanrieder et al. [4] (B) Experimental design combining in situ histochemistry with MALDI imaging MS, where the enzyme inhibitor is first added to one side of a normal control brain section, here at the level of the striatum. A substrate, dynorphin B (DynB), dissolved in ammonium acetate is added to all spots on both sides of the brain section before applying the MALDI matrix. Using MALDI imaging MS it is possible to detect the levels of substrate and peptide bioconversion products simultaneously, such as dynorphin B(2–13) at *m/z* 1408 and Leu-Enk-Arg (*m/z*712). The intensity of color reflects peak intensity in mass spectra. The enzyme inhibitor NEM (67 nanomol) almost completely blocked the des-tyrosination of dynorphin B and Leu-Enk-Arg (yellow box). Corpus callosum, cc; cortex, cx; striatum, str. (For interpretation of the references to color in this figure legend, the reader is referred to the web version of this article.)

and dynorphin neuropeptides after the development of L-DOPA-induced adverse drug effects (dyskinesia) in Parkinson's disease [2–5]. In previous studies we found that the levels of small dynorphins (dynorphin B and alpha-neoendorphin) in the parkinsonian striatum and substantia nigra were positively correlated with the severity of dyskinesia [4,5]. Although all dynorphins can bind and activate kappa opioid receptors, both dynorphin B and alpha-neoendorphin can interact with the other opiate receptors and in particular alpha-neoendorphin displays the least selectivity [6,7]. After release dynorphin peptides are bioconverted into shorter neuroactive fragments, sometimes targeting other receptors than the original parent peptide. In the rat model of Parkinson's disease, we have previously noted that in animals with a severe degree of motor adverse drug effects (dyskinesias) the des-tyrosination of the dynorphin peptides dynorphin A(1–8), dynorphin B, and alpha-neoendorphin is rapidly occurring in the striatum, but not the target structure substantia nigra (Fig. 1A) [4,5]. However, not much is known about the bioconversion of dynorphins *in vivo* and therefor dynorphin B was selected as the model neuropeptide in the current study [8,9].

Area-specific expression of CNS enzymes is known to modify the biological activity of several endogenous neuropeptides [8,10] and has recently been targeted for the development of novel drugs, for example for use in neuropathic pain [11–13]. Unbiased, rapid, and sensitive analytical tools to screen new drugs targeting enzymatic activity are important for finding drugs with high efficacy and therapeutic value.

This study focuses on establishing a fast and sensitive method with high-throughput capacity for screening enzyme inhibitors and their effects in different parts of the brain by combining *in situ*

histochemistry with MALDI imaging mass spectrometry. Prior to the introduction of immunohistochemistry, *in situ* histochemistry incubating a substrate often linked to a chromogen on fresh frozen tissue sections was the gold standard in pathology for the diagnosis of many diseases, including brain lesions, myocardial infarction, and celiac disease [14]. MALDI mass spectrometry has frequently been used for the detection of enzymatic activity, however to our knowledge there are no reports of using complex matrices such as tissue sections although this would often yield more biologically relevant information [15]. MALDI imaging MS is a versatile technique allowing unbiased (as no labeling is required) detection of many peptides and proteins simultaneously in the same biological tissue samples [16–18]. Here we add synthetic dynorphin B as our model substrate together with both general and more specific enzyme inhibitors, and map the peptide products in different parts of the brain using 2,5-dihydroxybenzoic acid (DHB) as a MALDI matrix as previously described [19,20].

2. Materials and methods

2.1. Animals, tissue preparation and ethical approval

Female 210–250 g Sprague-Dawley rats (Scanbur BK AB, Sweden), were used in this experiment. Animals were housed four to a cage with a 12:12 light/dark cycle with food and water *ad libitum*. The experiment was approved by the Uppsala animal ethics committee (no 140/8) and conducted in accordance with the guidelines of Swedish legislation on animal experimentation (Animal Welfare act SDS1998:56) and European Union Legislation (Convention ETS123 and Directive 86/609/EEC). The rats were deeply anesthetized with isoflurane and decapitated. The brains were immediately removed after death (<30 s) and frozen on finely ground dry ice.

2.2. MALDI imaging mass spectrometry

Rat brain sections (12 μm thick) were cut on a cryostat, mounted on indium-tin oxide (ITO)-coated slides (Bruker Daltonics, Germany) and stored at −20 °C until use. Unless otherwise stated, all chemicals were obtained from Sigma-Aldrich Co. (St. Louis, MO).

It is common to minimize the risk of interfering signals during MALDI analysis using ethanol washing; this was tested in a first experiment where tissue sections were washed once in 70% and twice in 95% ethanol (10 s and 2 times 10 s respectively) and compared with non-washed sections. No enhancement of signal was detected and the following experiments were carried out on non-washed sections. *N*-ethylmaleimide (NEM aminopeptidase inhibitor) were applied using micropipette (0,2 μL of 333 mM or 333 μM in 150 mM ammonium acetate (AmAc; pH 7; in LC–MS grade water) followed by dynorphin B peptide (2 pmol in 0.2 μL AmAc) and let dry at room temperature for 10 min before applying the MALDI matrix. The incubation time is thus limited to the 5–6 min it takes for the 0.2 μL dynorphin B in AmAc to dry completely and would be identical for all deposits across the experiment.

In order to establish a biologically effective concentration of specific inhibitors, six sections were microspotted as described above. The general inhibitor Protease Inhibitor Cocktail (PIC; Roche, Germany, ½ tablet in 5 mL AmAc), 10% acetic acid (HAc, in AmAc), and the inhibitors opiorphin (500 μM in AmAc) and phosphoramidon (100 μM in AmAc)) as well as vehicle (AmAc) alone were applied at three positions in cortex, one in dorsal and one in ventral striatum. The sections were allowed to dry before applying the dynorphin B substrate.

For micropipetted samples, matrix solution (0,2 μL of 25 mg/mL 2,5-di-hydroxybezoic acid (DHB) in 50% methanol, 40% water (LC–MS grade), 10% 150 mM AmAc and 0,3% trifluoroacetic acid (TFA) was applied twice. For imaging MS, dynorphin B (10 μM) alone or mixed with either opiorphin (500 μM) or phosphoramidon (100 μM), was applied at a resolution of 575 μm using a chemical inkjet printer (ChIP, Shimadzu, Japan). The solutions were applied at 50 drops per pass and 2 passes, and followed by matrix solution (20 drops per pass, 10 passes).

FlexImaging (Bruker Daltonics) was used to create the imaging sequence of micropipetted matrix spots, but because of the size and typical crystallization of DHB into ring like structures the mass spectra were collected manually (2000 shots collected for each spot) using a smart beam technology-equipped Ultraflex II (Burker Daltonics) operating in reflector positive mode. For printed arrays of DHB matrix, the size of each matrix deposit was close to the size of the laser beam and 800 shots per spot were collected in automatic mode. External calibration was performed with a standard peptide mix (Peptide Standard Calibration II, Bruker Daltonics). Baseline correction (Convex Hull) was performed for each individual spectrum and exported as dat-files using FlexAnalysis (Bruker Daltonics). Average mass spectra were created and analyzed in OriginPro (OriginLab Corporation, MA). If the total ion current of the experimental group did not differ from control group (DynB only) then a total ion current normalization was applied. The area under the curve was calculated for each dynorphin peak detected (signal-to-noise >3 and not present in control tissue without added dynorphin B) and used for statistics analysis. F-test analysis of variance revealed unequal variance between groups and the data was log-scaled for further analysis using ANOVA or Student's T-test (two-tailed, alpha 0.05, the null hypothesis was rejected at $P < 0.05$).

3. Results and discussion

High levels of endogenous dynorphin peptides are mainly localized to the ventral striatum in the normal intact rat striatum. In order to reliably detect dynorphin B in the ventral striatum it was necessary to increase the laser intensity at which point the synthetic dynorphin B saturated the detector, thus a lower laser intensity was chosen for the rest of the study. The difference between endogenous and exogenous applied dynorphin B was more than 4 orders of magnitude, making it impossible to visualize the endogenous dynorphins on the same scale in the images shown in the current study.

The concept of these experiments is to first apply the enzyme inhibitor to one side of normal intact brain, and then the substrate is deposited to both sides and allowed to dry (Fig. 1B). DHB matrix in an organic solution was applied and mass spectra were acquired using a MS imaging software in so-called profiling mode. First, a rather general inhibitor of proteases *N*-ethylmaleimide (NEM), that has been shown to inhibit dynorphin degradation in spinal cord [21], was chosen for the investigation of dynorphin B bioconversion at three sites in the normal intact brain; the cortex, the dorsal and ventral striatum.

Several proteolytic fragments were detected after addition of 2 pmol dynorphin B in the absence of NEM inhibitor and compared to a blank control. Dynorphin B(1–6; also called Leu-Enk-Arg), (1–9), (1–12), and (7–13) were the most abundant peptide products (Fig. 2, Supplemental Table 1). But in addition, dynorphin B (1–7; Leu-Enk-Arg-Arg), (1–8), (1–10), and the des-tyrosinated dynorphin B(2–13) could easily be detected in the striatum, whereas dynorphin B(1–5; Leu-Enk), (1–11), (4–13) and (6–13) displayed low intensities.

NEM (67 nmol) almost completely (>90%) blocked the conversion of dynorphin B to dynorphin B(1–6), (1–9), (2–13), and (7–13)

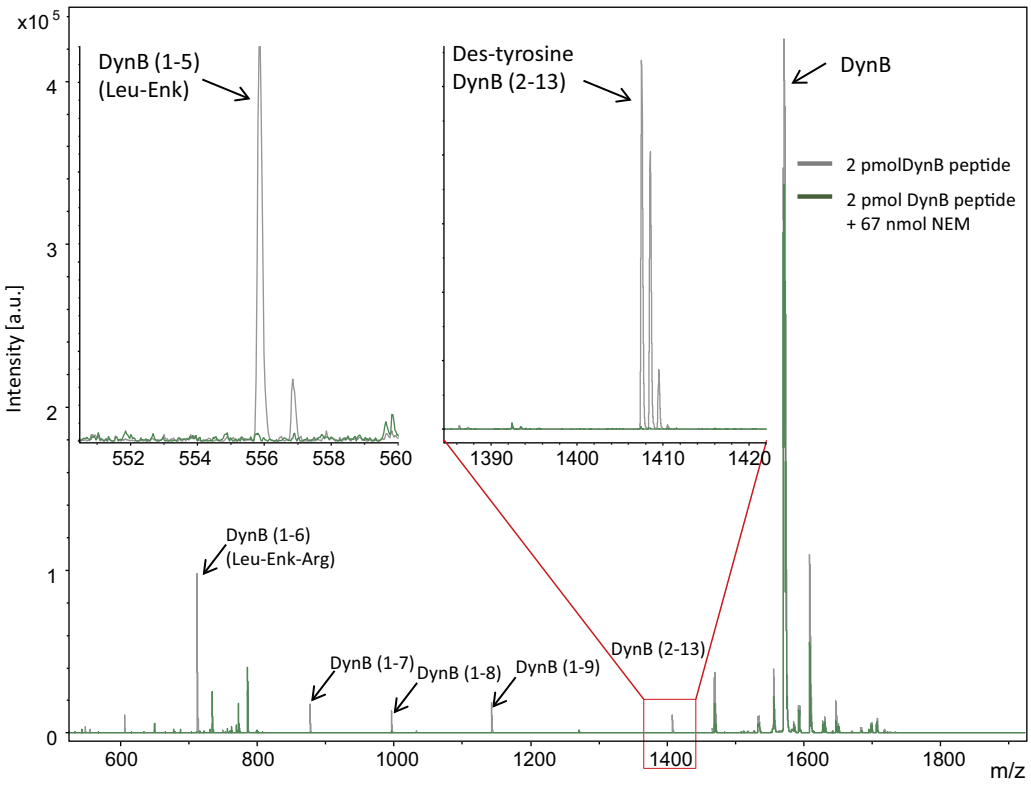

Fig. 2. Synthetic dynorphin B is bioconverted in native tissue sections and NEM blocks this conversion. Representative spectrum show the major peptide product fragments of dynorphin B bioconversion and that the enzyme inhibitor NEM (67 nanomol) almost completely blocked the bioconversion of dynorphin B (DynB) to Leu-Enk and the des-tyrosinated DynB(2–13) on native brain sections (green trace). Arrows point to the monoisotopic *m/z*. (For interpretation of the references to color in this figure legend, the reader is referred to the web version of this article.)

(Figs. 2 and 3, Supplemental Table 1; $p < 0.05$). In some cases the bioconversion of dynorphin B was only partially blocked by NEM, indicating activity of other non-cystein enzymes (Fig. 3; $p < 0.1$ but >0.05). Fewer C- than N-terminal peptide products were detected and the effect of NEM was more pronounced in the striatum compared with cortex. Lower amounts of NEM (67 pmol) only partially blocked the conversion of dynorphin B. The ion intensities of synthetic dynorphin B were almost the same in the presence and absence of NEM, suggesting that very little dynorphin B had been metabolized in this experiment (4% of peptide only group; Fig. 3 and Supplemental Table 1).

Brain tissue is known to contain salts that interfere with desorption and ionization of endogenous neuropeptides. Typically, a few brief washing steps (10 s in 70%, 95%, and 95% ethanol) are included in order to enhance the endogenous neuropeptide signals [19]. The ethanol washes did not increase the detection of the added dynorphin B and its products, thus only non-washed tissue was used for future experiments (data not shown). Another common concern is that the enzyme inhibitor causes ion suppression effects and thus produces false positive results. No ion suppression effects could be detected in the lower and higher molecular weight range (*m/z* 733 in Fig. 4; Supplemental Fig. 1). No in source fragmentation was detected from synthetic dynorphin B placed directly on a stainless steel target using the same acquisition method.

The combination of *in situ* histochemistry and MALDI imaging MS could be applied to both general inhibition of proteases and more specific inhibitors of peptidases. Unspecific inhibition of enzymatic activity by lowering the pH with acetic acid was the most effective strategy to block bioconversion of dynorphin B (Fig. 4). The majority of peptide product formation was blocked by acetic acid (ten out of twelve fragments) and about 60% more intact dynorphin B remained after acetic acid addition compared with dynorphin B alone and vehicle followed by dynorphin B. The proteinase inhibitor cocktail is a commercially available mix of many protease inhibitors, including for example aprotinin, bestatin, and leupeptin, and blocked the bioconversion into 4 peptide products by more than 60% and an additional 3 peptide products by about 30%.

Phosphoramidon (PA) is a metallo-endopeptidase inhibitor known to block the enkephalinase neprilysin (also called neutral endopeptidase, NEP; EC 3.4.24.11) in CNS. Recently, the similar phosphoramidon-sensitive NEP-2 has proven a critical amyloid-beta-degrading enzyme, causing plaque deposition when inhibited [22]. In neuropathic pain, the inhibition of neprilysin is used to increase the endogenous levels of opioids and alleviate pain [11–13]. Neprilysin mainly cleaves between two hydrophobic amino acids, and is known to cleave before the phenylalanine in position 4 of dynorphin B. Indeed, PA significantly reduced the formation of dynorphin B(4–13) by about 30% in the cortex and in addition blocked the formation of dynorphin B(1–10) by more than 60% in both striatum and cortex (Fig. 4). In neuropathic pain a novel concept targets both neprilysin and another enkephalinase: aminopeptidase N (ANPEP or APN1, EC 3.4.11.2), that is mainly responsible for removing the initial tyrosine that confer binding and activation of all endogenous opioid peptides to their receptor [11–13]. Opiorphin is a potent inhibitor of both aminopeptidase N and neprilysin, and has been implicated for treatment of neuropathic pain and cancer [11,23]. In the current study, opiorphin inhibited the formation of 5 dynorphin peptide products, including dynorphin B(2–13), (6–13), and (7–13) (Fig. 4).

Using a chemical ink-jet printer to apply inhibitor and substrate it is possible to analyze a large set of tissues rapidly and using much

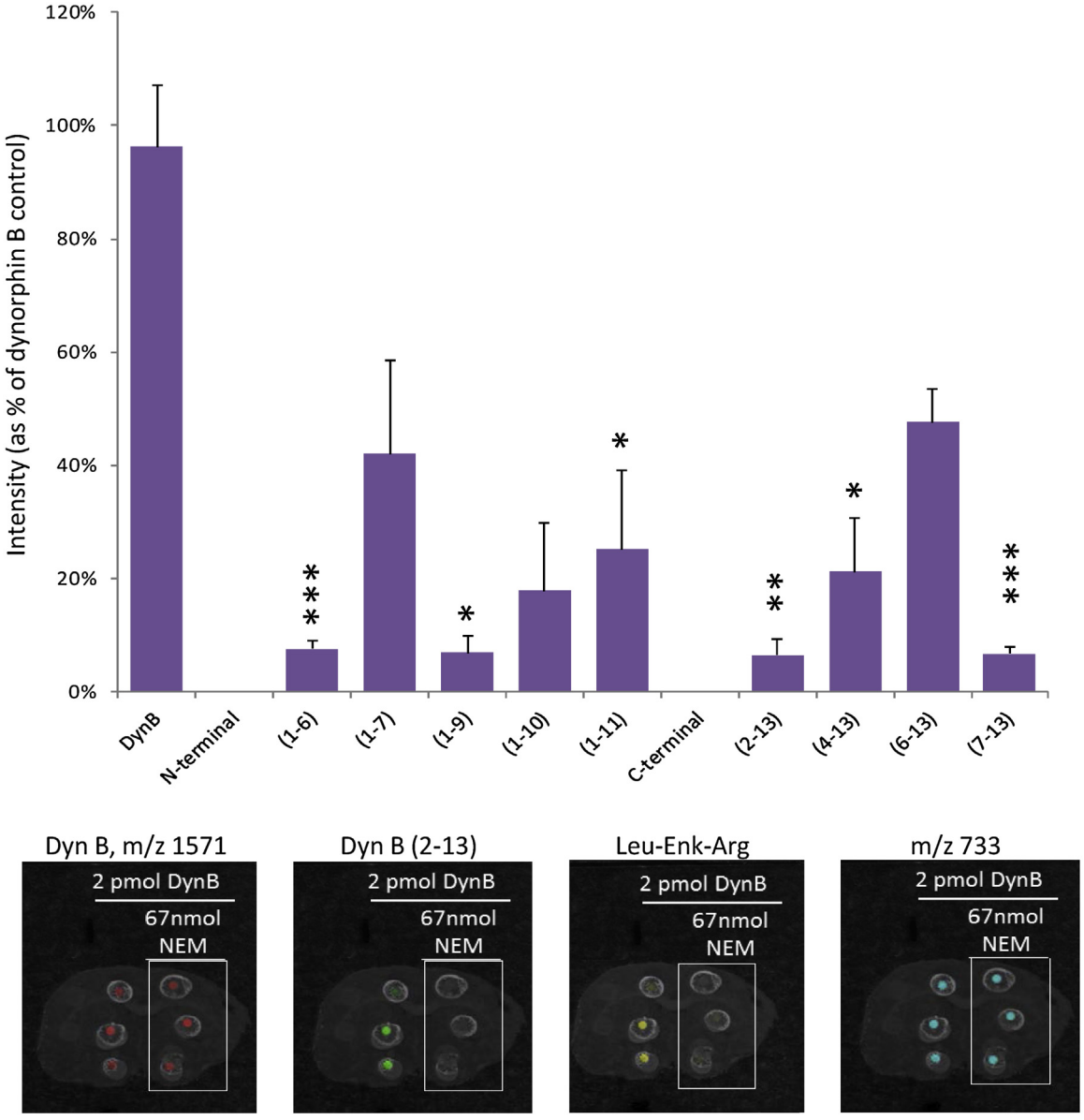

Fig. 3. Bioconversion into several peptide products blocked by NEM. Average intensity was measured as area under the curve and expressed as percent of synthetic dynorphin B (DynB) (average ± SEM of six matrix deposits in cortex, dorsal and ventral striatum). NEM had different effect on the conversion into each fragment. The formation of fragments (1–6), (1–9), (2–13), and (7–13) were blocked with more than 90%, whereas other fragments revealed only a partial block, and a few showed a trend towards significant block: dynorphin B (1–7; 1–10; 6–13; $p < 0.1$). The bottom panel demonstrates how a block of conversion into dynorphin B (2–13; 1–6) is visualized using the MALDI imaging MS software and where color intensity is reflecting peak height. Other molecular species were not affected by NEM, for example the unknown peak at *m/z* 733. This experiment was repeated once with similar results. *$p < 0.05$; **$p < 0.01$; ***$p < 0.001$.

smaller volumes (drop size 80 picoliter). In addition, this also makes it possible to print several iterations of either analyte or buffer in order to increase incubation time and enabling a more complete enzyme reaction, which has previously been shown for on-tissue protein trypsinization [20]. In the current study 100 fmol dynorphin B was applied to each spot in an array across a rat brain tissue section at the coronal level of striatum. On consecutive sections inhibitors were applied together with the substrate dynorphin B (a total of 5 pmol OPI or 1 pmol PA, with 100 fmol dynorphin B in each spot) and MALDI imaging MS acquired. Dynorphin B bioconversion displayed three distinct patterns; the most predominant was a homogenous bioconversion across all brain regions, however several fragments were enriched in the somatosensory cortex (for example dynorphin B(1–7)), and dynorphin B(2–13) showed especially high intensities in the striatum (Fig. 5). Opiorphin blocked formation of both these fragment, whereas phosphoramidon only blocked the formation of dynorphin B(1–7).

That enzyme activity is retained in native frozen sections is well known and that tissue preparation is important for imaging mass spectrometry has been shown in several studies [24,25]. Using this knowledge it has been possible to monitor degradation of endogenous phospholipids and proteins in a time-dependent manner using MALDI imaging MS [24,26]. Dynorphin bioconversion has previously been shown to differ between the striatum and substantia nigra, using either brain homogenates or microdialysis to infuse synthetic dynorphin and analyzing the collected dynorphin fragments using MALDI TOF MS [27–30]. For example, Prokai et al. noted a very similar bioconversion pattern to our results by incubating dynorphin A(1–8) with synaptosomes and synaptic membranes demonstrating bioconversion into dynorphin A (2–8), (1–6), and Leu-Enk. In addition, several groups have noted that

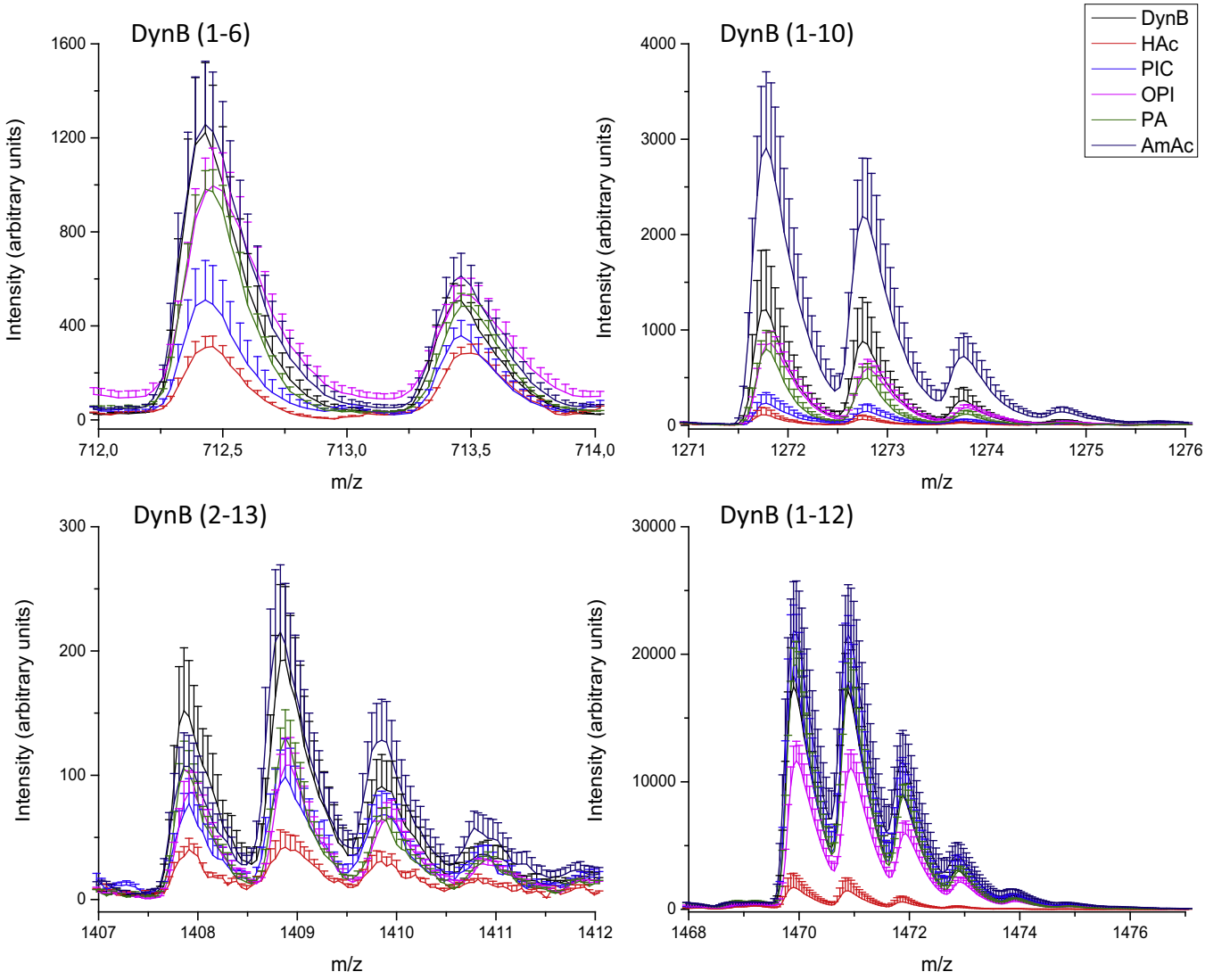

Fig. 4. Fast screening of general and more specific inhibitors. Average trace of matrix deposits placed in cortex and striatum show that lowering the pH using acetic acid (HAc) was the most effective way to inactivate endogenous enzymes in the native tissue sections. The commercially available proteinase inhibitor cocktail (PIC) was partially effective in preventing most, but not all peptide product fragments. The inhibitors opiorphin (OPI) and phosphoramidon (PA) displayed discrete effects that indicated a difference in effect between cortex and striatum when individual mass spectra were inspected (not shown). This experiment was conducted in less than a day, similar to the NEM experiment. Average trace of 4 or 5 matrix deposits per treatment ± SEM.

many synthetic dynorphins are rapidly converted into their des-tyrosine form both *in vivo* and *in vitro* [30–33]. However, using homogenates you have to have *a priori* knowledge of what specific areas contain the target enzyme, whereas using MALDI imaging MS you can screen entire sections for enzymatic activity. In addition, it is possible to target multiple areas using profiling/imaging MS in order to quickly assess enzyme activity levels in a high-throughput manner. Similarly, microdialysis studies require a large number of subjects and take a long time to perform compared to the experiment described here where hundreds of sections through a structure such as striatum can be obtained from one single animal. On the other hand, the microdialysis probe placement ensures that only the bioconversion of dynorphin in the extracellular space is measured, whereas the on-tissue histochemistry will reflect peptidase activity in all compartments similar to what is found using radioimmune assays.

Metabolism of dynorphin into shorter fragments is known to produce bioactive peptides that modulate neuronal signaling, sometimes interacting with receptors that do not recognize the parent peptides [8]. Bioconversion of this kind is not unique for opioid peptides, but has also been observed with substance P, nociceptin, and angiotensin II [10]. This has generated great interest in the development of enzyme inhibitors for the therapeutic potential of treatment of pain, addiction, depression, and other neurological diseases [9,21,34,35]. It is suspected that many bioconversion fragments have biologically important, but yet unknown functions. Indeed, a recent study comparing results from many peptidomics projects (using focused microwave irradiation to reduce post-mortem degradation of proteins and peptides) shows that the number of endogenous fragments is much larger than anticipated and postulates that this indicate their biological importance [36].

4. Conclusion

This proof-of-concept study demonstrates that it is possible to combine *in situ* histochemistry with unbiased analysis using MALDI imaging MS to rapidly screen the effect of enzyme inhibitors in different parts of the brain. This method can easily be adapted for other

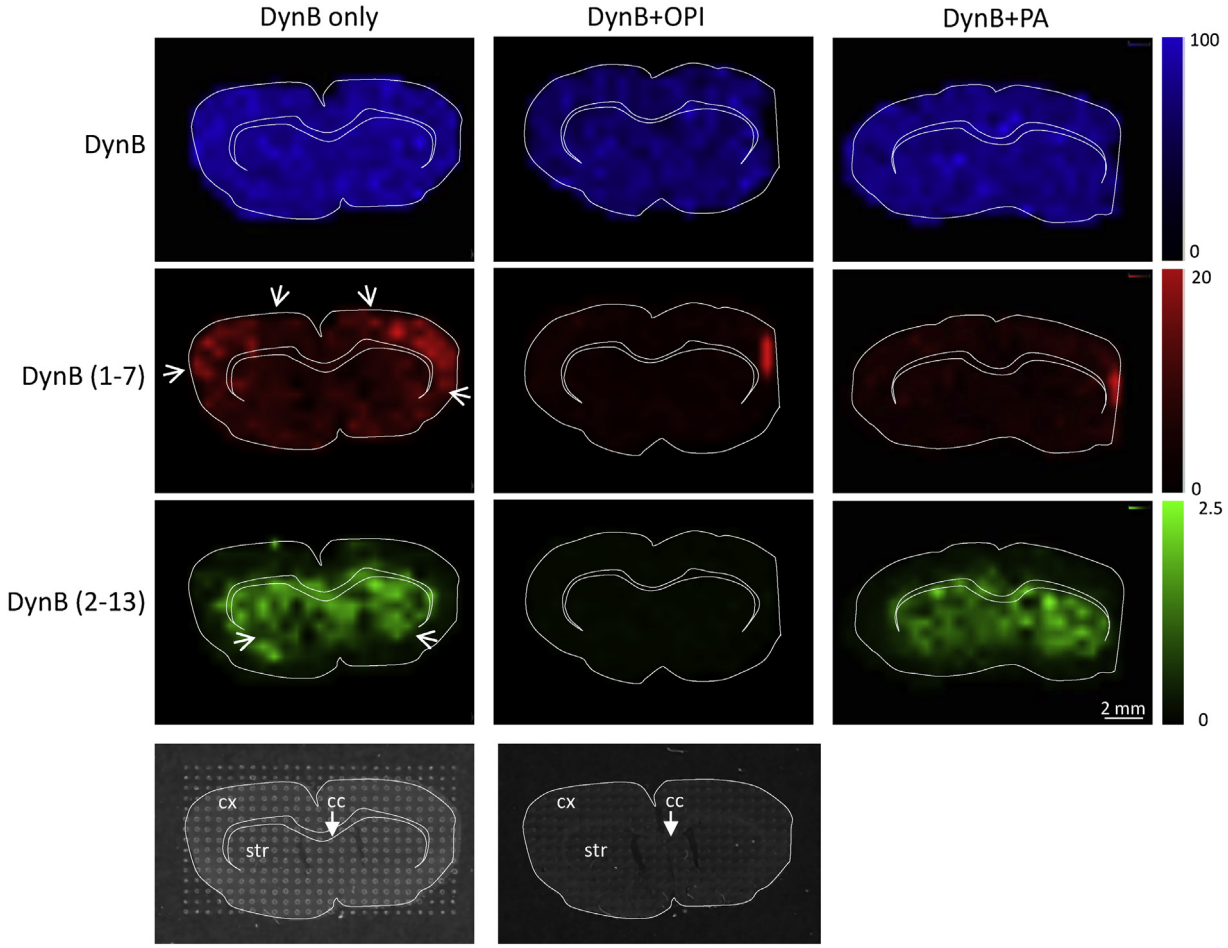

Fig. 5. Imaging MS reveals enzyme- and region-specific inhibition. Synthetic dynorphin B (100 fmol per matrix deposit) was generally bioconverted in both striatum and cortex to an equal extent. However, the dynorphin B (1–7) and (2–13) fragments displayed distinct localization to the somatosensory cortex (arrows in DynB(1–7)) and striatum (arrows in DynB(2–13), respectively. Opiorphin (OPI) effectively blocked the conversion into several fragments, including striatal dynorphin B (2–13), whereas phosphoramidon (PA) reduced cortical dynorphin B (1–7) and showed no effect on dynorphin B(2–13). A fold of the right edge of the tissue caused a mass shift that is detected as a lower signal in the DynB ion image and correspondingly an unknown ion light up in a few pixels in the DynB (1–7) ion images. After MS acquisition the matrix was washed off, revealing the underlying anatomical structures used for delineation of corpus callosum (cc) that separates cortex (cx) from striatum (str) (bottom panels; before and after matrix removal).

purposes and used for example in ADME studies for the detection of early signs of liver and kidney toxicity by measuring alkaline phosphatase activity *in situ* [14].

Additional information

Financial support was given by the Swedish Research Council grant #522-2006-6414 (MA), 521-2012-2304 (MA), 621-2011-4423 (JB), 342-2004-3944 (JB). This work was in part supported by grants from the Swedish Science Research Council (VR), and Swedish Research Council FORMAS (GB).

The authors have no competing financial interests. EB and RS carried out the experiments, interpreted the results, made figures and wrote the report. GB and JB provided materials and wrote the report. MA designed the experiments, interpreted the results, made figures, and wrote the report.

Acknowledgments

Ms Raili Engdahl and Lena Norgren are gratefully acknowledged for technical assistance and Dr. Tatiana Yakovleva for valuable input during the preparation of this manuscript. Prof. Eva Brittebo is thanked for donation of brain tissue sections.

Appendix A. Supplementary data

Supplementary data associated with this article can be found, in the online version, at http://dx.doi.org/10.1016/j.peptides.2016.11.006.

References

[1] F.M. Correa, L.M. Plunkett, J.M. Saavedra, Quantitative distribution of angiotensin-converting enzyme (kininase II) in discrete areas of the rat brain by autoradiography with computerized microdensitometry, Brain Res. 375 (1986) 259–266.
[2] M. Andersson, A. Hilbertson, M. Cenci, Striatal fosB expression is causally linked with l-DOPA-induced abnormal involuntary movements and the associated upregulation of striatal prodynorphin mRNA in a rat model of Parkinson's disease, Neurobiol. Dis. 6 (1999) 461–474.
[3] M.A. Cenci, C.S. Lee, A. Bjorklund, L-DOPA-induced dyskinesia in the rat is associated with striatal overexpression of prodynorphin- and glutamic acid decarboxylase mRNA, Eur. J. Neurosci. 10 (1998) 269–2706.
[4] J. Hanrieder, et al., L-DOPA-induced dyskinesia is associated with regional increase of striatal dynorphin peptides as elucidated by imaging mass spectrometry, Mol. Cell. Proteom. 10 (2011), http://dx.doi.org/10.1074/mcp.M111.009308, M111 009308.
[5] A. Ljungdahl, J. Hanrieder, M. Falth, J. Bergquist, M. Andersson, Imaging mass spectrometry reveals elevated nigral levels of dynorphin neuropeptides in L-DOPA-induced dyskinesia in rat model of Parkinson's disease, PLoS One 6 (2011) e25653, http://dx.doi.org/10.1371/journal.pone.0025653, PONE-D-11-04937 [pii].

[6] A. Mansour, M.T. Hoversten, L.P. Taylor, S.J. Watson, H. Akil, The cloned mu, delta and kappa receptors and their endogenous ligands: evidence for two opioid peptide recognition cores, Brain Res. 700 (1995) 89–98, 0006-8993(95)00928-J [pii].
[7] R. Schulz, M. Wuster, A. Herz, Endogenous ligands for kappa-opiate receptors, Peptides 3 (1982) 973–976.
[8] M. Hallberg, Neuropeptides: metabolism to bioactive fragments and the pharmacology of their receptors, Med. Res. Rev. 35 (2015) 464–519, http://dx.doi.org/10.1002/med.21323.
[9] J. Ner, J. Silberring, Dynorphin convertases and their functions in CNS, Curr. Pharm. Des. 19 (2013) 1043–1051.
[10] F. Nyberg, M. Hallberg, Peptide conversion—a potential pathway modulating G-protein signaling, Curr. Drug Targets 8 (2007) 147–154.
[11] B.P. Roques, M.C. Fournie-Zaluski, M. Wurm, Inhibiting the breakdown of endogenous opioids and cannabinoids to alleviate pain, Nat. Rev. Drug Discov. 11 (2012) 292–310, http://dx.doi.org/10.1038/nrd3673, nrd3673 [pii].
[12] H. Poras, E. Bonnard, E. Dange, M.C. Fournie-Zaluski, B.P. Roques, New orally active dual enkephalinase inhibitors (DENKIs) for central and peripheral pain treatment, J. Med. Chem. 57 (2014) 5748–5763, http://dx.doi.org/10.1021/jm500602h.
[13] E. Bonnard, et al., Long-lasting oral analgesic effects of N-protected aminophosphinic dual ENKephalinase inhibitors (DENKIs) in peripherally controlled pain, Pharmacol. Res. Perspect. 3 (2015) e00116, http://dx.doi.org/10.1002/prp2.116.
[14] W.A. Meier-Ruge, E. Bruder, Current concepts of enzyme histochemistry in modern pathology, Pathobiology 75 (2008) 233–243, http://dx.doi.org/10.1159/000132384.
[15] T. de Rond, M. Danielewicz, T. Northen, High throughput screening of enzyme activity with mass spectrometry imaging, Curr. Opin. Biotechnol. 31 (2015) 1–9, http://dx.doi.org/10.1016/j.copbio.2014.07.008.
[16] R.M. Caprioli, T.B. Farmer, J. Gile, Molecular imaging of biological samples: localization of peptides and proteins using MALDI-TOF MS, Anal. Chem. 69 (1997) 4751–4760.
[17] R.J. Goodwin, S.R. Pennington, A.R. Pitt, Protein and peptides in pictures: imaging with MALDI mass spectrometry, Proteomics 8 (2008) 3785–3800, http://dx.doi.org/10.1002/pmic.200800320.
[18] J.L. Norris, R.M. Caprioli, Analysis of tissue specimens by matrix-assisted laser desorption/ionization imaging mass spectrometry in biological and clinical research, Chem. Rev. 113 (2013) 2309–2342, http://dx.doi.org/10.1021/cr3004295.
[19] M. Andersson, M.R. Groseclose, A.Y. Deutch, R.M. Caprioli, Imaging mass spectrometry of proteins and peptides: 3D volume reconstruction, Nat. Methods 5 (2016) 101–108, http://dx.doi.org/10.1038/nmeth1145, nmeth1145 [pii].
[20] M.R. Groseclose, M. Andersson, W.M. Hardesty, R.M. Caprioli, Identification of proteins directly from tissue: in situ tryptic digestions coupled with imaging mass spectrometry, J. Mass Spectrom.: JMS 42 (2007) 254–262, http://dx.doi.org/10.1002/jms.1177.
[21] K. Tan-No, et al., Pronociceptive role of dynorphins in uninjured animals: *N*-ethylmaleimide-induced nociceptive behavior mediated through inhibition of dynorphin degradation, Pain 113 (2005) 301–309, http://dx.doi.org/10.1016/j.pain.2004.11.004.
[22] R.A. Marr, D.M. Hafez, Amyloid-beta and Alzheimer's disease: the role of neprilysin-2 in amyloid-beta clearance, Front. Aging Neurosci. 6 (2014) 187, http://dx.doi.org/10.3389/fnagi.2014.00187.
[23] M. Mizerska-Dudka, M. Kandefer-Szerszen, Opioids, neutral endopeptidase, its inhibitors and cancer: is there a relationship among them? Arch. Immunol. Ther. Exp. (Warsz) 63 (2015) 197–205, http://dx.doi.org/10.1007/s00005-014-0311-0.
[24] R.J. Goodwin, J.C. Dungworth, S.R. Cobb, A.R. Pitt, Time-dependent evolution of tissue markers by MALDI-MS imaging, Proteomics 8 (2008) 3801–3808, http://dx.doi.org/10.1002/pmic.200800201.
[25] R.J. Goodwin, S.L. Iverson, P.E. Andren, The significance of ambient-temperature on pharmaceutical and endogenous compound abundance and distribution in tissues sections when analyzed by matrix-assisted laser desorption/ionization mass spectrometry imaging, Rapid Commun. Mass Spectrom. 26 (2012) 494–498, http://dx.doi.org/10.1002/rcm.6125.
[26] N.H. Patterson, A. Thomas, P. Chaurand, Monitoring time-dependent degradation of phospholipids in sectioned tissues by MALDI imaging mass spectrometry, J. Mass Spectrom.: JMS 49 (2014) 622–627, http://dx.doi.org/10.1002/jms.3382.
[27] R. Klintenberg, P.E. Andren, Altered extracellular striatal in vivo biotransformation of the opioid neuropeptide dynorphin A(1–17) in the unilateral 6-OHDA rat model of Parkinson's disease, J. Mass Spectrom. 40 (2005) 261–270, http://dx.doi.org/10.1002/jms.754.
[28] K. Magnusson, M. Hallberg, J. Bergquist, F. Nyberg, Enzymatic conversion of dynorphin A in the rat brain is affected by administration of nandrolone decanoate, Peptides 28 (2007) 851–858, http://dx.doi.org/10.1016/j.peptides.2006.12.011.
[29] B. Reed, Y. Zhang, B.T. Chait, M.J. Kreek, Dynorphin A(1–17) biotransformation in striatum of freely moving rats using microdialysis and matrix-assisted laser desorption/ionization mass spectrometry, J. Neurochem. 86 (2003) 815–823, 1859 [pii].
[30] J. Sandin, et al., Differential metabolism of dynorphins in substantia nigra, striatum, and hippocampus, Peptides 18 (1997) 949–956, S0196-9781(97)00025-9 [pii].
[31] E.A. Young, J.M. Walker, R. Houghten, H. Akil, The degradation of dynorphin-A in brain-tissue in vivo and in vitro, Peptides 8 (1987) 701–707.
[32] I. Nylander, K. Tanno, A. Winter, J. Silberring, Processing of prodynorphin-derived peptides in striatal extracts—identification by electrospray–ionization mass spectrometry linked to size-exclusion chromatography, Life Sci. 57 (1995) 123–129.
[33] L. Prokai, A.D. Zharikova, Identification of synaptic metabolites of dynorphin A (1–8) by electrospray ionization and tandem mass spectrometry, Rapid Commun. Mass Spectrom. 12 (1998) 1796–1800.
[34] J. Ajimi, et al., Effect of three peptidase inhibitors on antinociceptive potential and toxicity with intracerebroventricular administration of dynorphin A (1–17) or (1–13) in the rat, J. Anesth. 29 (2015) 65–77, http://dx.doi.org/10.1007/s00540-014-1860-4.
[35] M. Morales-Mulia, P. de Gortari, M.I. Amaya, M. Mendez, Acute ethanol administration differentially alters enkephalinase and aminopeptidase N activity and mRNA levels in regions of the nigrostriatal pathway, J. Mol. Neurosci. 49 (2013) 289–300, http://dx.doi.org/10.1007/s12031-012-9823-4.
[36] L.D. Fricker, Analysis of mouse brain peptides using mass spectrometry-based peptidomics: implications for novel functions ranging from non-classical neuropeptides to microproteins, Mol. Biosyst. 6 (2010) 1355–1365, http://dx.doi.org/10.1039/c003317k.